



1 Anthropogenic aerosol forcing under the Shared Socioeconomic Pathways

2 Marianne T. Lund^{*,1}, Gunnar Myhre¹, Bjørn H. Samset¹

3 ¹ CICERO Center for International Climate Research, Oslo, Norway

4 ^{*}Corresponding author: Marianne T. Lund, m.t.lund@cicero.oslo.no

5

6 Abstract

7 Emissions of anthropogenic aerosols are expected to change drastically over the coming decades,
8 with potentially significant climate implications. Using the most recent generation of harmonized
9 emission scenarios, the Shared Socioeconomic Pathways (SSPs) as input to a global chemistry
10 transport and radiative transfer model, we provide estimates of the projected future global and
11 regional burdens and radiative forcing of anthropogenic aerosols under three different levels of air
12 pollution control: strong (SSP1), medium (SSP2) and weak (SSP3). We find that the broader range
13 of future air pollution emission trajectories spanned by the SSPs compared to previous scenarios
14 translates into total aerosol forcing estimates in 2100 relative to 1750 ranging from -0.04 W m^{-2} in
15 SSP1-1.9 to -0.51 W m^{-2} in SSP3-7.0. Compared to our 1750-2015 estimate of -0.61 W m^{-2} , this
16 shows that depending on the success of air pollution policies over the coming decades, aerosol
17 radiative forcing may weaken by nearly 95% or remain close to the pre-industrial to present-day
18 level. In all three scenarios there is a positive forcing in 2100 relative to 2015, from 0.51 W m^{-2} in
19 SSP1-1.9 to 0.04 W m^{-2} in SSP3-7.0. Results also demonstrate significant differences across
20 regions and scenarios, especially in South Asia and Africa. While rapid weakening of the negative
21 aerosol forcing following effective air quality policies will unmask more of the greenhouse gas-
22 induced global warming, slow progress on mitigating air pollution will significantly enhance the
23 atmospheric aerosol levels and risk to human health. In either case, the resulting impacts on
24 regional and global climate can be significant.

25

26 1 Introduction

27 Understanding the contribution of aerosols and other short-lived climate forcers to the total
28 anthropogenic radiative forcing (RF) is becoming increasingly important considering the
29 ambitious goals of the Paris Agreement. Under scenarios compliant with keeping global warming
30 below 1.5°C , global greenhouse gas emissions must generally be reduced to net zero by the middle
31 of the century, placing added focus on the evolution and relative importance of emissions of other
32 climate-relevant substances for the net future climate impact (IPCC, 2018). Additionally, aerosols
33 play a key role in shaping regional climate and environment, by modulating clouds, circulation
34 and precipitation and air quality. In South and East Asia, currently the largest emission source
35 regions, air pollution is one of the major health risks, estimated to have been responsible for 1.2
36 million deaths in 2017 in India alone (Balakrishnan et al., 2019). In the same region, aerosols may
37 have masked up to 1°C of surface warming (Samset, 2018), and the sensitivity of the regional
38 climate to reductions in aerosol emissions has been found to be high (Samset et al., 2018).



39 Several long-term scenarios for air pollutant emissions exist. Among the most recent examples are
40 the Representative Concentration Pathways (RCPs) (Granier et al., 2011). The RCPs formed the
41 basis for the Coupled Model Intercomparison Project Phase 5 (CMIP5) and have been used in a
42 number of studies to estimate the potential impact of future changes in aerosols on air quality and
43 health (e.g., Li et al., 2016; Partanen et al., 2018), radiative forcing and temperature (e.g., Chalmers
44 et al., 2012; Szopa et al., 2013; Westervelt et al., 2015) and precipitation and other climate
45 variables (Nazarenko et al., 2015; Pendergrass et al., 2015; Rotstayn et al., 2014).

46 The RCPs were developed to span a range of climate forcing levels and were not associated with
47 specific socio-economic narratives. The RCPs generally reflect the assumption that stringent air
48 quality regulations will be successfully implemented globally (Rao et al., 2017). As a result,
49 emissions of aerosols and aerosol precursors are projected to decline rapidly in all scenarios, even
50 under high forcing and greenhouse gas emission levels. However, despite efforts to control
51 pollutant emissions, ambient air quality continues to be a major concern in many parts of the world.
52 Global emissions of black and organic carbon (BC, OC) have increased rapidly over recent decades
53 (Hoesly et al., 2018). Global emissions of sulfur dioxide (SO₂) have declined, driven by legislation
54 in Europe and North America, the collapse of the former Soviet Union and, more recently, air
55 quality policies in China (Li et al., 2017; Zheng et al., 2018). However, in other regions of the
56 world, most notably South Asia, SO₂ emissions also continue to be high and increasing. The slow
57 progress on alleviating air pollution, raises the question of whether previous projections of future
58 emissions are too optimistic in terms of pollution control. More recent scenario development has
59 included alternative assumptions to better understand the mechanisms and interlinkages with
60 reference scenarios and climate policy co-benefits (Chuwah et al., 2013; Rao et al., 2013; Rogelj
61 et al., 2014). These provide a wider range of possible developments but are still largely
62 independent of underlying narratives.

63 To provide a framework for combining future climate scenarios with socioeconomic development,
64 the Shared Socioeconomic Pathways (SSPs) (O'Neill et al., 2014) were produced. The SSPs
65 provide five narratives for plausible future evolution of society and natural systems in the absence
66 of climate change and combine these with seven different climate forcing targets using integrated
67 assessment modeling, building a matrix of emission scenarios with socioeconomic conditions on
68 one axis and climate change on the other. Associated projections of air pollution emissions have
69 been developed, where three different assumptions for future pollution control (strong, medium
70 and weak) based on characteristics of control targets, rate of implementation of effective policies
71 and technological progress are mapped to specific SSPs (Rao et al., 2017). In the strong pollution
72 control scenarios (SSP1 and SSP5), increasing health and environmental concerns result in lower
73 than current emission levels in the medium to long term. A similar, but slower development is seen
74 under medium control (SSP2), whereas under weak control (SSP3 and SSP4) there is progress is
75 slowed and regionally fragmented. This results in a broad range in projected emission in the
76 baseline marker scenarios, with the highest emissions in SSP3, followed by SSP4, and the lowest
77 in SSP1 or SSP5 (Rao et al., 2017).



78 Here we use three of the scenarios as input to a global chemical transport model and offline
79 radiative transfer calculations (Sect. 2) in order to quantify the future evolution of aerosols under
80 strong, medium and weak air pollution control. We present results for both global and regional
81 developments in aerosol loadings and radiative forcing (Sec. 3) and discuss implications of the
82 findings in the context of previous generation emission scenarios and outlooks for more detailed
83 studies of the wider climate implications of potential air quality policies (Sect. 4). Conclusions are
84 given in Sect.5.

85

86 2 Method

87 Atmospheric concentrations of aerosols are simulated with the OsloCTM3 (Søvde et al., 2012).
88 The OsloCTM3 is a global, offline chemistry-transport model driven by meteorological forecast
89 data from the European Center for Medium Range Weather Forecast (ECMWF) OpenIFS model.
90 Here the model is run in a $2.25^\circ \times 2.25^\circ$ horizontal resolution using fixed meteorological data for
91 2010. The present-day aerosol distributions simulated by the OsloCTM3 were recently
92 documented and evaluated by Lund et al. (2018). We refer to the same paper for detailed
93 descriptions about the aerosol modules and treatment of scavenging and transport in the
94 OsloCTM3.

95 Simulations with SSP air pollution emissions are performed for the years 2015, 2020, 2030, 2050
96 and 2100, keeping the meteorology fixed. Specifically, we use the IMAGE (van Vuuren et al.,
97 2017) SSP1-1.9, MESSAGE-GLOBIOM (Fricko et al., 2017) SSP2-4.5 and AIM (Fujimori et al.,
98 2017) SSP3-7.0 scenarios. Gridded data for each scenario has been harmonized with the
99 Community Emission Data System (CEDS) historical emissions (Gidden et al., 2019) and are
100 available via Earth System Grid Federation (ESGF) by the Integrated Assessment Modeling
101 Consortium (IAMC). Several additional SSPs exist, but these largely fall in the range between
102 SSP1 and SSP3. Each simulation is run for 18 months, discarding the first six as spin-up. Natural
103 emission sources (soil, ocean, vegetation) are kept at the present-day level and the data sets
104 described in Lund et al. (2018). See Sect. 4 Discussion for comments on the potential implications
105 of this choice.

106 Using the same model setup as in the present study, Lund et al. (2018) recently calculated the
107 historical (1750-2014) evolution of aerosols following the Community Emission Data System
108 (CEDS) inventory (Hoesly et al., 2018). The future projections from the present study are
109 combined with this historical time series. Furthermore, whereas Lund et al. (2018) only assessed
110 the direct aerosol RF, we here include an estimate of the radiative forcing due to aerosol-cloud
111 interactions.

112 We calculate the instantaneous top-of-the atmosphere radiative forcing due to aerosol-radiation
113 interactions (RFari) (Myhre et al., 2013b) using offline radiative transfer calculations with a multi-
114 stream model using the discrete ordinate method (Stamnes et al., 1988). The same model has been
115 used in earlier studies of RFari (Myhre et al., 2017; Myhre et al., 2013a) with some small recent



116 updates to aerosol optical properties (Lund et al., 2018). The radiative forcing of aerosol-cloud
117 interactions (RF_{aci}) (earlier denoted as the cloud albedo effect or Twomey effect) is calculated
118 using the same radiative transfer model. To account for the change in cloud droplet concentration
119 resulting from anthropogenic aerosols, which alter the cloud effective radius and thus the optical
120 properties of the clouds, the approach from Quaas et al. (2006) is used. This method has also been
121 applied in earlier studies (Myhre et al., 2017).

122

123 3 Results

124 In the following, we first document the future global emissions and abundances of aerosols,
125 according to our three chosen SSPs. We then show the resulting regional aerosol burden levels,
126 and finally global and regional radiative forcing. For simplicity we refer to SSP1-1.9 as SSP1,
127 SSP2-4.5 as SSP2 and SSP3-7.0 as SSP3 throughout the text.

128 Figure 1a-d shows annual global emissions (fossil fuel, biofuel and biomass burning) of BC, OC,
129 SO₂ and nitrogen oxides (NO_x) from 1950 to 2100 in the CEDS inventory and the SSPs used in
130 the present analysis. For comparison, we also include the RCP2.6 (van Vuuren et al., 2007),
131 RCP4.5 (Smith & Wigley, 2006) and RCP8.5 (Riahi et al., 2007) 2015-2100 emissions. Total
132 emissions excluding biomass burning are shown in Fig. S1. For all four species, the temporal
133 evolution and difference between scenarios have the similar characteristics. In SSP1 (strong air
134 pollution control), emissions are projected to decline from 2015. This decline is particularly rapid
135 for BC and SO₂, with emissions falling to around 25% of their 2015 levels already by 2040. For
136 NO_x and OC, emissions are projected to go down by around 80% by the end of the century. Apart
137 from SO₂, SSP3 (weak air pollution control) sees an increase in emissions by towards the mid-21st
138 century (by 10-20% above 2015 levels), followed by a decline back to, or slightly below the
139 present-day by 2100. Emissions in SSP2 (medium air pollution control) follow an intermediate
140 pathway; a decline throughout the century, but less steep and with a higher end-of-century levels
141 than SSP1. As a result of the homogeneous underlying assumptions about the level of air pollution
142 mitigation, the RCPs display much smaller spread and emissions fall throughout the century. All
143 three RCPs generally lie between SSP1 and SSP2. There is also a decline in biomass burning
144 emissions in SSP1 and SSP2, where emissions are around 30%-40% lower in 2100 compared to
145 2015. Rao et al. (2017) note that changes in biomass burning emissions are not necessarily driven
146 by air pollution policies but can be linked to assumptions about the land-use sector in the respective
147 integrated assessment models.

148 The rapidly decreasing anthropogenic emissions in SSP1 result in global total burdens (Fig. 1e-h)
149 of BC, primary organic aerosol (POA) and sulfate that are 30%, 45% and 60%, respectively, of
150 the present-day level by 2100. Under this pathway, biomass burning sources becomes relatively
151 more important over the century: fossil fuel and biofuel emissions constitute 70% of the total BC
152 burden in 2015, but only 36% by 2100. Similar end-of-century changes are found under SSP2, but
153 in this case the decline mainly occurs after 2050. In SSP3, the global aerosol burdens increase
154 toward the mid-century followed by a small or negligible change to 2100 compared to 2015. The



155 global burden of nitrate is twice as high in 2100 compared to 2015 in SSP3. This is due to the
156 combination of increased global ammonia (NH_3) emissions (not shown), which are 30% higher by
157 2100, a small net change in NO_x emissions and a decrease in SO_2 emissions, resulting in less
158 competition for available ammonia by sulfate aerosols. The potentially more important role of
159 nitrate aerosols under certain emission pathways has been documented in previous studies as well
160 (Bauer et al., 2007; Bellouin et al., 2011). In SSP1 and SSP2, there is negligible net change in NH_3
161 emissions over the century, while NO_x emissions decline, resulting in a lower burden also of
162 nitrate. Figure 1i-j shows the simulated anthropogenic global-mean aerosol optical depth (AOD)
163 and absorption aerosol optical depth (AAOD) (calculated as the difference between each year and
164 the 1750 value as the meteorology and hence contribution from natural aerosols is constant). The
165 anthropogenic AOD falls from 0.026 in 2015 to 0.0005 in 2100 in SSP1 and 0.006 in SSP2. These
166 changes correspond to a reduction of the total AOD of 20% (15%) in 2100 in SSP1 (SSP2) from
167 the present-day level of 0.13. In SSP3, the anthropogenic AOD increases by 12% to 2050 before
168 returning approximately to its present-day value. Similar magnitude decreases in anthropogenic
169 AAOD are found. The decline in anthropogenic AOD is stronger than implied by the burden
170 changes. We note that the sulfate and nitrate burdens include also smaller contributions from
171 natural (ocean and vegetation) sources that remain constant to 2100. In SSP1 we find a small,
172 negative AAOD value in 2100. This results from emissions on BC and OC being lower in 2100
173 than in 1750. The stronger decline in anthropogenic AAOD relative to AOD in SSP1 is reflected
174 in the total (anthropogenic and natural aerosols) Single Scattering Albedo (SSA) (Fig. 1k) which
175 increases to above pre-1970s levels by mid-century and is notably higher than in SSP3 by the end
176 of the century. As the mechanisms that link aerosol emissions to climate impacts are markedly
177 different for scattering and absorbing aerosols (Ocko et al., 2014; Samset et al., 2016; Smith et al.,
178 2018), this reduction highlights a need for regional studies of aerosol impacts that go beyond the
179 total top-of-atmosphere effective radiative forcing.

180 The global-mean time series hide significant spatiotemporal differences in aerosol trends. Figure
181 2 shows the time series of the BC and sulfate burdens, the two dominant species, averaged across
182 9 regions: North America (NAM), Europe (EUR), Russia (RBU), East Asia (EAS), South Asia
183 (SAS), South East Asia (SEA), North Africa and the Middle East (NAF_MDE), South Africa (SAF)
184 and South America (SAM). The well-known geographical shift in historical emission is clearly
185 reflected, where the largest aerosols loadings were located over North America, Europe and Russia
186 in the 1970s and 80s, but later peaking over Asia. In the coming decades, the South and East Asia
187 will continue to experience the highest aerosol loadings under SSP2 and SSP3. However, towards
188 the end of the century North Africa and the Middle East reaches similar levels. Africa south of
189 Sahara is presently the third largest BC emission source region (Fig. S2). Under SSP3,
190 anthropogenic (fossil and biofuel) emissions are projected to increase strongly over the century in
191 Africa south of Sahara and the region surpasses East Asia as the largest source in 2100, although
192 levels stay below current emission levels in China. Figure 2 shows that a slightly decreasing BC
193 burden is projected over the region in all three SSPs. In this case, the increase in fossil fuel
194 emissions is offset by a decrease in biomass burning emissions, which constitute a significant
195 fraction of the total BC source here. Despite lower emissions in the latter, BC burdens in southern
196 and northern parts of Africa are of the same order of magnitude. One reason for this is likely
197 differing scavenging pathways, where aerosols are more effectively removed, and the atmospheric



198 residence time is shorter, further south. Moreover, we note that the regionally averaged burden
199 does not directly link to regional emissions, as they are also influenced by long-range transport.
200 Using multi-model data from the Hemispheric Transport of Air Pollution (HTAP2) experiments,
201 studies have demonstrated while for most receptor regions, within-region emissions dominates,
202 there are the important contribution from long-range transport from e.g., Asia to aerosols over
203 North America, Middle East and Russia (e.g., Liang et al., 2018; Stjern et al., 2016; Tan et al.,
204 2018). Hence, the projected emission changes in this region can have far reaching impacts.

205 The radiative forcing of anthropogenic aerosols relative to 1750 is shown for the period 1950 to
206 2100 in Fig. 3, for RFari, RFaci, and the total aerosol RF (RFtotal), separately. Results from the
207 present study are complimented by results based on simulations from Lund et al. (2018) (see
208 Methods) for the historical period. We calculate a net aerosol-induced RF in 2014, relative to 1750,
209 of -0.61 W m^{-2} , whereof -0.17 W m^{-2} is due to aerosol-radiation interactions, as also shown in
210 Lund et al. (2018), and -0.44 W m^{-2} due to aerosol-cloud interactions. Due to the rapid emission
211 reductions projected over the next couple of decades, the RF is less than half in magnitude to its
212 present-day value in SSP1 already by 2030, continuing to weaken at a slower rate after. In 2100,
213 the RFtotal is -0.04 W m^{-2} in SSP1 and -0.20 W m^{-2} in SSP2. With emissions following SSP3, the
214 temporal evolution of RF is nearly flat through the 21st century and is -0.51 W m^{-2} in 2100, only
215 15% lower in magnitude than in 2014. Even with weak air pollution control (SSP3) end-of-the-
216 century emissions are slightly lower than the present-day level. Hence, looking only at the period
217 2015-2100, we estimate a positive aerosol forcing in all three scenarios considered. The RFtotal
218 in 2100 relative to 2015 is 0.51 W m^{-2} , 0.35 W m^{-2} and 0.04 W m^{-2} in SSP1, SSP2 and SSP3,
219 respectively. The estimates presented here do not account for the rapid adjustments (or semi-direct
220 effects) associated with BC, which has been suggested to offset a significant fraction of the positive
221 BC RFari, resulting a lower than previously found net impact of BC aerosols (Stjern et al., 2017).

222 Few modeling-based estimates for comparison with our results exist so far. In a recent study,
223 Fiedler et al. (2019b) used a simple plume parameterization of optical properties and cloud effects
224 of anthropogenic aerosols and scaled the present-day aerosol optical depth by the SSP emissions
225 to derive estimates of future forcing. An effective radiative forcing (ERF) (comparable to our
226 RFtotal) ranging from -0.15 W m^{-2} for SSP1-1.9 to -0.54 W m^{-2} for SSP3-7.0 was calculated.
227 This is in reasonable agreement with the estimates derived in the present analysis, although we
228 find a weaker forcing in SSP1. Using two idealized scenarios to span a broader range of emissions
229 than represented in the RCPs, Partanen et al. (2018) also estimated a broad range in aerosol ERF,
230 from -0.02 W m^{-2} to -0.82 W m^{-2} , in 2100. The latter is significantly stronger than our SSP3
231 estimate. While not directly comparable due to differing emission inventories and methodologies,
232 these studies reinforce our finding that weak air pollution control over the 21st century result in
233 sustained strong negative aerosol forcing.

234 The spatiotemporal differences in trend documented above translates into effects on global and
235 regional RF. In Fig. 4 we therefore show the change in RFtotal over four time periods, 1750-2015,
236 1750-1990, 1990-2015 and 2015-2030 (for each SSP). Figure S3 show the corresponding results
237 for RFari and RFaci separately. Whereas the impact of anthropogenic aerosols is a negative RFtotal
238 everywhere except over the high-albedo deserts and snow-covered regions when taken over the
239 entire historical period 1750-2015, a positive RF is found seen over North America, Europe and



240 Russia after the 1990–2015 period, driven by decreased SO₂ emissions (and somewhat offset by a
241 simultaneous decline in BC emissions). This positive RF is largely driven by aerosol–radiation
242 interactions. Over South and East Asia, Africa and most of South America the RF_{total} remains
243 negative, although a significant fraction of the total impact since pre-industrial has already been
244 realized before 1990. This weaker negative forcing is due to a combination of increasing BC
245 emissions and a leveling off in SO₂ emissions in China in the CEDS inventory (Hoesly et al. 2018).
246 Globally, the combined effect is an increase in global-mean RF_{total} over the 1990–2015 period of
247 +0.09 W m⁻². Using the ECLIPSE emission inventory, (Myhre et al., 2017) estimated an increase
248 in the multi-model RF due to combined changes in aerosols and ozone from 1990 to 2015 of +0.17
249 W m⁻², with about two-thirds of this from aerosols, i.e., similar to our results using the CEDS/SSP
250 emissions.

251 Distinct regional differences are seen also during the period 2015–2030 under the different SSPs.
252 With emissions following SSP1, we estimate a positive global-mean RF_{total} of 0.33 W m⁻², more
253 than three times the RF_{total} over the 1990–2015 period. In contrast to the 1990–2015 period, the
254 strongest RF now comes from aerosol–cloud interactions, as emissions over continental northern
255 hemisphere regions are low to begin with. The RF_{total} is especially large over South and East Asia,
256 and of opposite sign from what the region has experienced during the past decades. Smaller
257 positive global mean RF_{total} of 0.08 W m⁻² is estimated also under SSP2 and SSP3 during this
258 period. In contrast to SSP1, the RF remains negative over India under SSP2 and SSP3 where a
259 continued increase in emissions of SO₂ is projected over the next decades. In all SSPs, the RF_{total}
260 over China switches from negative in the past decades to positive over the 2015–2030 period.
261 Recent studies suggest that Chinese SO₂ emissions have declined even more than captured by the
262 CEDS until 2014, indicating that this pattern of forcing may already have been partly realized (Li
263 et al., 2017; Zheng et al., 2018). In contrast, emissions of India are projected to increase, at least
264 initially. The potential implications of this feature are discussed in a separate paper (Samset et al.,
265 2019). Weak RF is found over the African continent in the SSP2 and 3 scenarios. However, as
266 shown in Figure 2, aerosols will continue to affect local climate and air quality in this region.

267

268 4 Discussion

269 Under a given scenario, emissions of all species follow the same general trend, although the rate
270 of change differs between regions. However, over the recent years, emissions of SO₂ have declined,
271 whereas BC emissions have increased (Hoesly et al., 2018). Considering a hypothetical case where
272 the mainly industrial, and perhaps easier to mitigate SO₂ emissions begin to decline rapidly also
273 in other high emitting regions, whereas the mainly residential, and therefore more challenging, BC
274 sources remain largely unchecked, the aerosol forcing may follow a different path than estimated
275 here. As an illustrative example, we calculate the contribution to RF_{ari} in 2020 and 2050 (relative
276 to 1750) from individual components under SSP1 and SSP3 (Table S1). Taking the sum of the
277 sulfate forcing from SSP1 and the remaining components from SSP3, the total RF_{ari} is -0.018 W
278 m⁻² in 2020, i.e., significantly weaker than when all emissions follow SSP1, and 0.15 W m⁻² in
279 2050. Hence, continuing along the recent emission development could mean a net positive direct
280 aerosol effect relative to pre-industrial, at least towards the mid-century, adding to the greenhouse



281 gas induced warming. As noted above, this does not, however, account for the rapid adjustments
282 which have been shown to reduce the global surface temperature response to BC perturbations.

283 We present projected future aerosol RF based on single-model simulations. Aerosols, however,
284 remain one of the most uncertain drivers of climate change, with significant model spread resulting
285 from several factors, including differences in the simulated aerosol distributions, optical properties
286 and cloud fields. Myhre et al. (2013a) calculated a present-day aerosol RF_{ari} (relative to 1850)
287 varying from -0.016 W m^{-2} to -0.58 W m^{-2} between 16 global models participating in the AeroCom
288 Phase II experiment. Prescribing the distribution of anthropogenic aerosols, optical properties and
289 effect on cloud droplet number concentration in six Earth System Models, Fiedler et al. (2019a)
290 find a model spread in aerosol ERF of -0.4 W m^{-2} to -0.9 W m^{-2} . Among the important
291 consequences of high aerosol forcing uncertainty is the challenge it poses for estimating climate
292 sensitivity. While in a scenario with declining aerosol emissions, combined with an increase in
293 greenhouse gases, the uncertainty in the total anthropogenic forcing can be expected to decrease
294 substantially even without scientific progress (Myhre et al., 2015), the high emission SSP3
295 pathway suggest that aerosols may continue to be a confounding factor for constraining climate
296 sensitivity.

297 While the scope of the present analysis is limited to radiative forcing, the calculated spread in end-
298 of-century forcing under the SSPs will translate into a wide range of possible climate impacts. A
299 number of studies have examined the future aerosol-induced radiative forcing and climate impacts
300 using the RCP projections; see e.g., Westervelt et al. (2015) for a summary of papers published
301 until 2013. While the magnitude of both present-day and future estimates differs between studies,
302 the general characteristic is a significant weakening of the aerosol RF until 2100 in all scenarios.
303 Other studies have investigated the potential for this rapid decline to drive near-term warming
304 (Chalmers et al., 2012; Gillett & Von Salzen, 2013). However, while Chalmers et al. (2012) find
305 a higher near-term warming in RCP2.6 than in RCP4.5 despite lower greenhouse gas forcing in
306 the former, suggesting an important impact of falling aerosol emissions, Gillett and Von Salzen
307 (2013) find no evidence that aerosol emissions reductions drive a particularly rapid near-term
308 warming in this scenario. Under SSP1, aerosol emissions are projected to decline even more
309 rapidly than in RCP2.6 over the coming couple of decades (Fig. 1). If in fact associated with a
310 rapid warming, this development could further hinder the realization of the already ambitious
311 temperature goals of the Paris agreement and this feature hence needs to be better quantified.
312 Previous work also demonstrate effects of falling aerosol emissions also other climate variables
313 such as mean and extreme precipitation (Navarro et al., 2017; Pendergrass et al., 2015) and
314 atmospheric dynamics (Rotstayn et al., 2014). The numerous and significant impacts of aerosols
315 underline the need to encompass the full range of projected emissions, regionally and globally, in
316 future assessment, in particular in light of the crucial role of aerosols in shaping regional climate,
317 regional assessments are needed to capture the impact of different trends.

318 It is well-established that future changes in aerosols will critically affect local air quality. Partanen
319 et al. (2018) estimated almost 80% fewer PM_{2.5}-induced deaths per year in 2100 under RCP4.5



320 compared to 2010. Conversely, an idealized high aerosol scenario resulted in 17% increase in
321 premature mortality by 2030. These numbers were estimated using present-day population
322 density. Under all SSPs, considerable increases in population density is projected in Africa, the
323 Middle East and South Asia (Jones & O'Neill, 2016) – regions that are also identified as hotspots
324 for exposure and vulnerability to multi-sector climate risk (Byers et al., 2018). In the present study,
325 we estimate an increase in the average surface concentration of anthropogenic aerosols (i.e., BC,
326 POA, sulfate and fine mode nitrate) of 17% and 25% by 2100 under SSP3 in South Asia and North
327 Africa plus the Middle East, respectively. Air pollution issues are not limited to developing
328 countries. While all scenarios project reductions in surface aerosol concentrations in Europe, North
329 America and Russia, there are substantial differences in the magnitude, from 35-20% lower by
330 2100 in SSP3 to around 70% lower in SSP1, highlighting the potential for stringent policies to
331 impose air quality improvements globally.

332 Our study does not account for potential impacts of climate change on circulation, precipitation or
333 chemistry, which can affect the lifetime and transport pathways, as well as emissions, of the
334 aerosols. For instance, Bellouin et al. (2011) found increasing atmospheric residence times over
335 the 21st century as wet deposition rates decreased. Including both changing climate and emissions,
336 Pommier et al. (2018) suggested that concentrations of particulate matter (PM_{2.5}) will increase by
337 up to 6.5% over the Indo-Gangetic Plain to 2050, driven by increases in dust, particulate organic
338 matter and secondary inorganic aerosols through changes in precipitation, biogenic emissions and
339 wind speed. Hence, by keeping natural sources of emissions fixed at present-day levels, our results
340 may underestimate the future aerosols loads. Moreover, a recent review of climate feedbacks on
341 aerosol distributions suggests that in regions where anthropogenic aerosol loadings decrease, the
342 impacts of climate on the variability of natural aerosols increase (Tegen & Schepanski, 2018).
343 Changing climatic conditions may also affect the radiative forcing through changing cloud
344 distributions and surface albedo. While our approach clearly disentangles and assesses the changes
345 in aerosols resulting from changes in anthropogenic emissions, representation and knowledge of
346 feedback processes are important for understanding the full role of future aerosols in the climate
347 system.

348

349 5 Conclusions

350 Using a global chemistry transport model and radiative transfer modeling, we have estimated the
351 projected future loading and radiative forcing of anthropogenic aerosols under the most recent
352 generation of scenarios, the Shared Socioeconomic Pathways. These new air pollution scenarios
353 link varying degrees of air pollution control to the socioeconomic narratives underlying the SSPs,
354 spanning a much broader range of plausible future emission trajectories than previous scenarios.
355 Here we have used three scenarios: SSP3-7.0 (weak air pollution control), SSP2-4.5 (medium
356 pollution control) and SSP1-1.9 (strong pollution control). In all three scenarios, we estimate a
357 positive aerosol forcing over the period 2015-2100, although with very different timing and
358 magnitude depending on stringency of air pollution control. The end-of-century aerosol forcing
359 relative to 2015 is 0.51 W m⁻² with emissions following SSP1, 0.35 W m⁻² in SSP2 and 0.04 W m⁻²



360 ² in SSP3. While effective air pollution control and socioeconomic development following SSP1
361 results in a rapid weakening of the aerosol RF compared to the pre-industrial to present-day level
362 already by 2030, there is little change in the global mean aerosol forcing over the 21st century in a
363 regionally fragmented world with slower mitigation progress. Significant spatiotemporal
364 differences in trends are also highlighted. Most notably, under weak air pollution control, aerosol
365 loadings in East and South Asia temporarily increases from present levels but starts to decline after
366 2050 and return to current levels of slightly below by 2100. North Africa and the Middle East
367 reaches the levels of South Asia by the end of the century and there is no declining trend this
368 century. The present analysis is limited to the documentation of radiative forcing and aerosol loads.
369 Under both rapidly declining and sustained high emissions, aerosols will play an important role in
370 shaping and affect regional and global climate.

371

372 Code availability

373 Oslo CTM3 is stored in a SVN repository at the University of Oslo central subversion system
374 and is available upon request. Please contact m.t.lund@cicero.oslo.no. In this paper, we use the
375 official version 1.0, Oslo CTM3 v1.0.

376

377 Data availability

378 The gridded SSP anthropogenic emission data are published within the ESGF system [https://esgf-](https://esgf-node.llnl.gov/search/input4mips/)
379 [node.llnl.gov/search/](https://esgf-node.llnl.gov/search/input4mips/) input4mips/ (last access: December 2018). Model output and post-processing
380 routines are available upon request from Marianne T. Lund (m.t.lund@cicero.oslo.no).

381

382 Author contributions

383 MTL performed the Oslo CTM3 experiments and led the analysis and writing. GM performed the
384 radiative transfer modeling and BHS contributed with graphics production. All authors contributed
385 during the writing of the paper.

386

387

388 Acknowledgements

389 The authors acknowledge funding from the Norwegian Research Council through grants 248834
390 (QUISARC) and 240372 (AC/BC). We also acknowledge the Research Council of Norway's
391 programme for supercomputing (NOTUR).

392

393 Competing interests

394 The authors declare that they have no conflict of interest.

395

396



397 References

- 398 Balakrishnan K., Dey S., Gupta T., Dhaliwal R. S., Brauer M., Cohen A. J., Stanaway J. D., Beig
399 G., Joshi T. K., Aggarwal A. N., Sabde Y., Sadhu H., Frostad J., Causey K., Godwin W., Shukla D. K.,
400 Kumar G. A., Varghese C. M., Muraleedharan P., Agrawal A., Anjana R. M., Bhansali A., Bhardwaj D.,
401 Burkart K., Cercy K., Chakma J. K., Chowdhury S., Christopher D. J., Dutta E., Furtado M., Ghosh S.,
402 Ghoshal A. G., Glenn S. D., Guleria R., Gupta R., Jeemon P., Kant R., Kant S., Kaur T., Koul P. A.,
403 Krish V., Krishna B., Larson S. L., Madhipatla K., Mahesh P. A., Mohan V., Mukhopadhyay S., Mutreja
404 P., Naik N., Nair S., Nguyen G., Odell C. M., Pandian J. D., Prabhakaran D., Prabhakaran P., Roy A.,
405 Salvi S., Sambandam S., Saraf D., Sharma M., Shrivastava A., Singh V., Tandon N., Thomas N. J., Torre
406 A., Xavier D., Yadav G., Singh S., Shekhar C., Vos T., Dandona R., Reddy K. S., Lim S. S., Murray C. J.
407 L., Venkatesh S. & Dandona L.: The impact of air pollution on deaths, disease burden, and life
408 expectancy across the states of India: the Global Burden of Disease Study 2017, *The Lancet Planetary*
409 *Health*. 3(1), e26-e39, [https://doi.org/10.1016/S2542-5196\(18\)30261-4](https://doi.org/10.1016/S2542-5196(18)30261-4), 2019.
- 410 Bauer S. E., Koch D., Unger N., Metzger S. M., Shindell D. T. & Streets D. G.: Nitrate aerosols
411 today and in 2030: a global simulation including aerosols and tropospheric ozone, *Atmospheric*
412 *Chemistry and Physics*. 7(19), 5043-5059, 2007.
- 413 Bellouin N., Rae J., Jones A., Johnson C., Haywood J. & Boucher O.: Aerosol forcing in the
414 Climate Model Intercomparison Project (CMIP5) simulations by HadGEM2-ES and the role of
415 ammonium nitrate, *Journal of Geophysical Research-Atmospheres*. 116, D20206, 10.1029/2011jd016074,
416 2011.
- 417 Byers E., Gidden M., Leclère D., Balkovic J., Burek P., Ebi K., Greve P., Grey D., Havlik P.,
418 Hillers A., Johnson N., Kahil T., Krey V., Langan S., Nakicenovic N., Novak R., Obersteiner M.,
419 Pachauri S., Palazzo A., Parkinson S., Rao N. D., Rogelj J., Satoh Y., Wada Y., Willaerts B. & Riahi K.:
420 Global exposure and vulnerability to multi-sector development and climate change hotspots,
421 *Environmental Research Letters*. 13(5), 055012, 10.1088/1748-9326/aabf45, 2018.
- 422 Chalmers N., Highwood E. J., Hawkins E., Sutton R. & Wilcox L. J.: Aerosol contribution to the
423 rapid warming of near-term climate under RCP 2.6, *Geophysical Research Letters*. 39(18),
424 doi:10.1029/2012GL052848, 2012.
- 425 Chuwah C., van Noije T., van Vuuren D. P., Hazeleger W., Strunk A., Deetman S., Beltran A. M.
426 & van Vliet J.: Implications of alternative assumptions regarding future air pollution control in scenarios
427 similar to the Representative Concentration Pathways, *Atmospheric Environment*. 79, 787-801,
428 <https://doi.org/10.1016/j.atmosenv.2013.07.008>, 2013.
- 429 Fiedler S., Kinne S., Huang W. T. K., Räisänen P., O'Donnell D., Bellouin N., Stier P., Merikanto
430 J., van Noije T., Makkonen R. & Lohmann U.: Anthropogenic aerosol forcing – insights from multiple
431 estimates from aerosol-climate models with reduced complexity, *Atmos. Chem. Phys.* 19(10), 6821-6841,
432 10.5194/acp-19-6821-2019, 2019a.
- 433 Fiedler S., Stevens B., Gidden M., Smith S. J., Riahi K. & van Vuuren D.: First forcing estimates
434 from the future CMIP6 scenarios of anthropogenic aerosol optical properties and an associated Twomey
435 effect, *Geosci. Model Dev.* 12(3), 989-1007, 10.5194/gmd-12-989-2019, 2019b.
- 436 Fricko O., Havlik P., Rogelj J., Klimont Z., Gusti M., Johnson N., Kolp P., Strubegger M., Valin
437 H., Amann M., Ermolieva T., Forsell N., Herrero M., Heyes C., Kindermann G., Krey V., McCollum D.
438 L., Obersteiner M., Pachauri S., Rao S., Schmid E., Schoepp W. & Riahi K.: The marker quantification of
439 the Shared Socioeconomic Pathway 2: A middle-of-the-road scenario for the 21st century, *Global*
440 *Environmental Change*. 42, 251-267, <https://doi.org/10.1016/j.gloenvcha.2016.06.004>, 2017.
- 441 Fujimori S., Hasegawa T., Masui T., Takahashi K., Herran D. S., Dai H., Hijioka Y. & Kainuma
442 M.: SSP3: AIM implementation of Shared Socioeconomic Pathways, *Global Environmental Change*. 42,
443 268-283, <https://doi.org/10.1016/j.gloenvcha.2016.06.009>, 2017.
- 444 Gidden M. J., Riahi K., Smith S. J., Fujimori S., Luderer G., Kriegler E., van Vuuren D. P., van
445 den Berg M., Feng L., Klein D., Calvin K., Doelman J. C., Frank S., Fricko O., Harmsen M., Hasegawa
446 T., Havlik P., Hilaire J., Hoesly R., Horing J., Popp A., Stehfest E. & Takahashi K.: Global emissions



- 447 pathways under different socioeconomic scenarios for use in CMIP6: a dataset of harmonized emissions
448 trajectories through the end of the century, *Geosci. Model Dev.* 12(4), 1443-1475, 10.5194/gmd-12-1443-
449 2019, 2019.
- 450 Gillett N. P. & Von Salzen K.: The role of reduced aerosol precursor emissions in driving near-
451 term warming, *Environmental Research Letters.* 8(3), 034008, 10.1088/1748-9326/8/3/034008, 2013.
- 452 Granier C., Bessagnet B., Bond T., D'Angiola A., Denier van der Gon H., Frost G. J., Heil A.,
453 Kaiser J. W., Kinne S., Klimont Z., Kloster S., Lamarque J.-F., Liousse C., Masui T., Meleux F., Mieville
454 A., Ohara T., Raut J.-C., Riahi K., Schultz M. G., Smith S. J., Thompson A., van Aardenne J., van der
455 Werf G. R. & van Vuuren D. P.: Evolution of anthropogenic and biomass burning emissions of air
456 pollutants at global and regional scales during the 1980–2010 period, *Climatic Change.* 109(1), 163,
457 10.1007/s10584-011-0154-1, 2011.
- 458 Hoesly R. M., Smith S. J., Feng L., Klimont Z., Janssens-Maenhout G., Pitkanen T., Seibert J. J.,
459 Vu L., Andres R. J., Bolt R. M., Bond T. C., Dawidowski L., Kholod N., Kurokawa J. I., Li M., Liu L.,
460 Lu Z., Moura M. C. P., O'Rourke P. R. & Zhang Q.: Historical (1750–2014) anthropogenic emissions of
461 reactive gases and aerosols from the Community Emission Data System (CEDS), *Geosci. Model Dev.*
462 2018(11), 369-408, <https://doi.org/10.5194/gmd-11-369-2018>, 2018.
- 463 IPCC: Summary for Policymakers. In: *Global warming of 1.5°C. An IPCC Special Report on the*
464 *impacts of global warming of 1.5°C above pre-industrial levels and related global greenhouse gas*
465 *emission pathways, in the context of strengthening the global response to the threat of climate change,*
466 *sustainable development, and efforts to eradicate poverty* [V. Masson-Delmotte, P. Zhai, H. O. Pörtner,
467 D. Roberts, J. Skea, P. R. Shukla, A. Pirani, W. Moufouma-Okia, C. Péan, R. Pidcock, S. Connors, J. B.
468 R. Matthews, Y. Chen, X. Zhou, M. I. Gomis, E. Lonnoy, T. Maycock, M. Tignor, T. Waterfield (eds.)].
469 World Meteorological Organization, Geneva, Switzerland, 32 pp., 2018.
- 470 Jones B. & O'Neill B. C.: Spatially explicit global population scenarios consistent with the
471 Shared Socioeconomic Pathways, *Environmental Research Letters.* 11(8), 084003, 10.1088/1748-
472 9326/11/8/084003, 2016.
- 473 Li C., McLinden C., Fioletov V., Krotkov N., Carn S., Joiner J., Streets D., He H., Ren X., Li Z.
474 & Dickerson R. R.: India Is Overtaking China as the World's Largest Emitter of Anthropogenic Sulfur
475 Dioxide, *Scientific Reports.* 7(1), 14304, 10.1038/s41598-017-14639-8, 2017.
- 476 Li K., Liao H., Zhu J. & Moch J. M.: Implications of RCP emissions on future PM_{2.5} air quality
477 and direct radiative forcing over China, *Journal of Geophysical Research: Atmospheres.* 121(21), 12,985-
478 913,008, doi:10.1002/2016JD025623, 2016.
- 479 Liang C. K., West J. J., Silva R. A., Bian H., Chin M., Davila Y., Dentener F. J., Emmons L.,
480 Flemming J., Folberth G., Henze D., Im U., Jonson J. E., Keating T. J., Kucsera T., Lenzen A., Lin M.,
481 Lund M. T., Pan X., Park R. J., Pierce R. B., Sekiya T., Sudo K. & Takemura T.: HTAP2 multi-model
482 estimates of premature human mortality due to intercontinental transport of air pollution and emission
483 sectors, *Atmos. Chem. Phys.* 18(14), 10497-10520, 10.5194/acp-18-10497-2018, 2018.
- 484 Lund M. T., Myhre G., Haslerud A. S., Skeie R. B., Griesfeller J., Platt S. M., Kumar R., Myhre
485 C. L. & Schulz M.: Concentrations and radiative forcing of anthropogenic aerosols from 1750 to 2014
486 simulated with the Oslo CTM3 and CEDS emission inventory, *Geosci. Model Dev.* 11(12), 4909-4931,
487 10.5194/gmd-11-4909-2018, 2018.
- 488 Myhre G., Samset B. H., Schulz M., Balkanski Y., Bauer S., Berntsen T. K., Bian H., Bellouin
489 N., Chin M., Diehl T., Easter R. C., Feichter J., Ghan S. J., Hauglustaine D., Iversen T., Kinne S.,
490 Kirkevåg A., Lamarque J. F., Lin G., Liu X., Lund M. T., Luo G., Ma X., van Noije T., Penner J. E.,
491 Rasch P. J., Ruiz A., Seland Ø., Skeie R. B., Stier P., Takemura T., Tsigaridis K., Wang P., Wang Z., Xu
492 L., Yu H., Yu F., Yoon J. H., Zhang K., Zhang H. & Zhou C.: Radiative forcing of the direct aerosol
493 effect from AeroCom Phase II simulations, *Atmos. Chem. Phys.* 13(4), 1853-1877, 10.5194/acp-13-1853-
494 2013, 2013a.
- 495 Myhre G., Shindell D., Brèon F.-M., Collins W., Fuglestedt J., Huang J., Koch D., Lamarque J.-
496 F., Lee D., Mendoza B., Nakajima T., Robock A., Stephens G., Takemura T. & Zhang H.: Anthropogenic
497 and natural radiative forcing. In: *Climate Change 2013: The Physical Science Basis. Contribution of*



- 498 Working Group I to the Fifth Assessment Report of the Intergovernmental Panel on Climate Change
499 [Stocker, T.F., D., Qin, G.-K. Plattner, M. Tignor, S.K. Allen, J. Boschung, A. Nauels, Y. Xia, V. Bex
500 and P.M. Midgley (eds). Cambridge University Press, Cambridge, United Kingdom and New York, NY,
501 USA 2013b.
- 502 Myhre G., Boucher O., Bréon F.-M., Forster P. & Shindell D.: Declining uncertainty in transient
503 climate response as CO₂ forcing dominates future climate change, *Nature Geoscience*. 8, 181,
504 10.1038/ngeo2371
- 505 <https://www.nature.com/articles/ngeo2371#supplementary-information>, 2015.
- 506 Myhre G., Aas W., Cherian R., Collins W., Faluvegi G., Flanner M., Forster P., Hodnebrog Ø.,
507 Klimont Z., Lund M. T., Mülmenstädt J., Lund Myhre C., Olivie D., Prather M., Quaas J., Samset B. H.,
508 Schnell J. L., Schulz M., Shindell D., Skeie R. B., Takemura T. & Tsyro S.: Multi-model simulations of
509 aerosol and ozone radiative forcing due to anthropogenic emission changes during the period 1990–2015,
510 *Atmos. Chem. Phys.* 17(4), 2709–2720, 10.5194/acp-17-2709-2017, 2017.
- 511 Navarro J. C. A., Ekman A. M. L., Pausata F. S. R., Lewinschal A., Varma V., Seland Ø., Gauss
512 M., Iversen T., Kirkevåg A., Riipinen I. & Hansson H. C.: Future Response of Temperature and
513 Precipitation to Reduced Aerosol Emissions as Compared with Increased Greenhouse Gas
514 Concentrations, *Journal of Climate*. 30(3), 939–954, 10.1175/jcli-d-16-0466.1, 2017.
- 515 Nazarenko L., Schmidt G. A., Miller R. L., Tausnev N., Kelley M., Ruedy R., Russell G. L.,
516 Aleinov I., Bauer M., Bauer S., Bleck R., Canuto V., Cheng Y., Clune T. L., Del Genio A. D., Faluvegi
517 G., Hansen J. E., Healy R. J., Kiang N. Y., Koch D., Lacis A. A., LeGrande A. N., Lerner J., Lo K. K.,
518 Menon S., Oinas V., Perlwitz J., Puma M. J., Rind D., Romanou A., Sato M., Shindell D. T., Sun S.,
519 Tsigaridis K., Unger N., Voulgarakis A., Yao M.-S. & Zhang J.: Future climate change under RCP
520 emission scenarios with GISS ModelE2, *Journal of Advances in Modeling Earth Systems*. 7(1), 244–267,
521 doi:10.1002/2014MS000403, 2015.
- 522 O'Neill B. C., Kriegler E., Riahi K., Ebi K. L., Hallegatte S., Carter T. R., Mathur R. & van
523 Vuuren D. P.: A new scenario framework for climate change research: the concept of shared
524 socioeconomic pathways, *Climatic Change*. 122(3), 387–400, 10.1007/s10584-013-0905-2, 2014.
- 525 Ocko I. B., Ramaswamy V. & Ming Y.: Contrasting Climate Responses to the Scattering and
526 Absorbing Features of Anthropogenic Aerosol Forcings, *Journal of Climate*. 27(14), 5329–5345,
527 10.1175/jcli-d-13-00401.1, 2014.
- 528 Partanen A.-I., Landry J.-S. & Matthews H. D.: Climate and health implications of future aerosol
529 emission scenarios, *Environmental Research Letters*. 13(2), 024028, 10.1088/1748-9326/aaa511, 2018.
- 530 Pendergrass A. G., Lehner F., Sanderson B. M. & Xu Y.: Does extreme precipitation intensity
531 depend on the emissions scenario?, *Geophysical Research Letters*. 42(20), 8767–8774,
532 doi:10.1002/2015GL065854, 2015.
- 533 Pommier M., Fagerli H., Gauss M., Simpson D., Sharma S., Sinha V., Ghude S. D., Landgren O.,
534 Nyiri A. & Wind P.: Impact of regional climate change and future emission scenarios on surface O₃ and
535 PM_{2.5} over India, *Atmos. Chem. Phys.* 18(1), 103–127, 10.5194/acp-18-103-2018, 2018.
- 536 Quaas J., Boucher O. & Lohmann U.: Constraining the total aerosol indirect effect in the LMDZ
537 and ECHAM4 GCMs using MODIS satellite data, *Atmos. Chem. Phys.* 6(4), 947–955, 10.5194/acp-6-
538 947-2006, 2006.
- 539 Rao S., Pachauri S., Dentener F., Kinney P., Klimont Z., Riahi K. & Schoepp W.: Better air for
540 better health: Forging synergies in policies for energy access, climate change and air pollution, *Global
541 Environmental Change*. 23(5), 1122–1130, <https://doi.org/10.1016/j.gloenvcha.2013.05.003>, 2013.
- 542 Rao S., Klimont Z., Smith S. J., Van Dingenen R., Dentener F., Bouwman L., Riahi K., Amann
543 M., Bodirsky B. L., van Vuuren D. P., Aleluia Reis L., Calvin K., Drouet L., Fricko O., Fujimori S.,
544 Gernaat D., Havlik P., Harmsen M., Hasegawa T., Heyes C., Hilaire J., Luderer G., Masui T., Stehfest E.,
545 Strefler J., van der Sluis S. & Tavoni M.: Future air pollution in the Shared Socio-economic Pathways,
546 *Global Environmental Change*. 42, 346–358, <https://doi.org/10.1016/j.gloenvcha.2016.05.012>, 2017.



- 547 Riahi K., Grübler A. & Nakicenovic N.: Scenarios of long-term socio-economic and
548 environmental development under climate stabilization, *Technological Forecasting and Social Change*.
549 74(7), 887-935, <https://doi.org/10.1016/j.techfore.2006.05.026>, 2007.
- 550 Rogelj J., Rao S., McCollum D. L., Pachauri S., Klimont Z., Krey V. & Riahi K.: Air-pollution
551 emission ranges consistent with the representative concentration pathways, *Nature Climate Change*. 4,
552 446, 10.1038/nclimate2178
- 553 <https://www.nature.com/articles/nclimate2178#supplementary-information>, 2014.
- 554 Rotstayn L. D., Plymin E. L., Collier M. A., Boucher O., Dufresne J.-L., Luo J.-J., Salzen K. v.,
555 Jeffrey S. J., Foujols M.-A., Ming Y. & Horowitz L. W.: Declining Aerosols in CMIP5 Projections:
556 Effects on Atmospheric Temperature Structure and Midlatitude Jets, *Journal of Climate*. 27(18), 6960-
557 6977, 10.1175/jcli-d-14-00258.1, 2014.
- 558 Samset B. H., Myhre G., Forster P. M., Hodnebrog Ø., Andrews T., Faluvegi G., Fläschner D.,
559 Kasoar M., Kharin V., Kirkevåg A., Lamarque J.-F., Olivie D., Richardson T., Shindell D., Shine K. P.,
560 Takemura T. & Voulgarakis A.: Fast and slow precipitation responses to individual climate forcers: A
561 PDRMIP multimodel study, *Geophysical Research Letters*. 43(6), 2782-2791, 10.1002/2016gl068064,
562 2016.
- 563 Samset B. H.: How cleaner air changes the climate, *Science*. 360(6385), 148-150,
564 10.1126/science.aat1723, 2018.
- 565 Samset B. H., Sand M., Smith C. J., Bauer S. E., Forster P. M., Fuglestedt J. S., Osprey S. &
566 Schleussner C.-F.: Climate Impacts From a Removal of Anthropogenic Aerosol Emissions, *Geophysical*
567 *Research Letters*. 45(2), 1020-1029, doi:10.1002/2017GL076079, 2018.
- 568 Samset B. H., Lund M. T., Bollasina M., Wilcox L. & Myhre G.: Rapidly emerging patterns of
569 Asian aerosol forcing, *Nature Geoscience* (in revision) 2019.
- 570 Smith C. J., Kramer R. J., Myhre G., Forster P. M., Soden B. J., Andrews T., Boucher O.,
571 Faluvegi G., Fläschner D., Hodnebrog Ø., Kasoar M., Kharin V., Kirkevåg A., Lamarque J.-F.,
572 Mühlenthaler J., Olivie D., Richardson T., Samset B. H., Shindell D., Stier P., Takemura T., Voulgarakis
573 A. & Watson-Parris D.: Understanding Rapid Adjustments to Diverse Forcing Agents, *Geophysical*
574 *Research Letters*. 45(21), 12,023-012,031, 10.1029/2018gl079826, 2018.
- 575 Smith S. J. & Wigley T. M. L.: Multi-Gas Forcing Stabilization with Minicam, *The Energy*
576 *Journal*. 27, 373-391, 2006.
- 577 Stamnes K., Tsay S. C., Wiscombe W. & Jayaweera K.: Numerically stable algorithm for
578 discrete-ordinate-method radiative transfer in multiple scattering and emitting layered media, *Appl. Opt.*
579 27(12), 2502-2509, 10.1364/AO.27.002502, 1988.
- 580 Stjern C. W., Samset B. H., Myhre G., Bian H., Chin M., Davila Y., Dentener F., Emmons L.,
581 Flemming J., Haslerud A. S., Henze D., Jonson J. E., Kucsera T., Lund M. T., Schulz M., Sudo K.,
582 Takemura T. & Tilmes S.: Global and regional radiative forcing from 20 % reductions in BC, OC and
583 SO₄ – an HTAP2 multi-model study, *Atmos. Chem. Phys.* 16(21), 13579-13599, 10.5194/acp-16-13579-
584 2016, 2016.
- 585 Stjern C. W., Samset B. H., Myhre G., Forster P. M., Hodnebrog Ø., Andrews T., Boucher O.,
586 Faluvegi G., Iversen T., Kasoar M., Kharin V., Kirkevåg A., Lamarque J.-F., Olivie D., Richardson T.,
587 Shawki D., Shindell D., Smith C. J., Takemura T. & Voulgarakis A.: Rapid Adjustments Cause Weak
588 Surface Temperature Response to Increased Black Carbon Concentrations, *Journal of Geophysical*
589 *Research: Atmospheres*. 122(21), 11,462-411,481, 10.1002/2017JD027326, 2017.
- 590 Szopa S., Balkanski Y., Schulz M., Bekki S., Cugnet D., Fortems-Cheiney A., Turquety S., Cozic
591 A., Déandréis C., Hauglustaine D., Idelkadi A., Lathière J., Lefevre F., Marchand M., Vuolo R., Yan N.
592 & Dufresne J.-L.: Aerosol and ozone changes as forcing for climate evolution between 1850 and 2100,
593 *Climate Dynamics*. 40(9), 2223-2250, 10.1007/s00382-012-1408-y, 2013.
- 594 Søvde O. A., Prather M. J., Isaksen I. S. A., Berntsen T. K., Stordal F., Zhu X., Holmes C. D. &
595 Hsu J.: The chemical transport model Oslo CTM3, *Geosci. Model Dev.* 5(6), 1441-1469, 10.5194/gmd-5-
596 1441-2012, 2012.



597 Tan J., Fu J. S., Dentener F., Sun J., Emmons L., Tilmes S., Flemming J., Takemura T., Bian H.,
598 Zhu Q., Yang C. E. & Keating T.: Source contributions to sulfur and nitrogen deposition – an HTAP II
599 multi-model study on hemispheric transport, *Atmos. Chem. Phys.* 18(16), 12223-12240, 10.5194/acp-18-
600 12223-2018, 2018.

601 Tegen I. & Schepanski K.: Climate Feedback on Aerosol Emission and Atmospheric
602 Concentrations, *Current Climate Change Reports.* 4(1), 1-10, 10.1007/s40641-018-0086-1, 2018.

603 van Vuuren D. P., den Elzen M. G. J., Lucas P. L., Eickhout B., Strengers B. J., van Ruijven B.,
604 Wonink S. & van Houdt R.: Stabilizing greenhouse gas concentrations at low levels: an assessment of
605 reduction strategies and costs, *Climatic Change.* 81(2), 119-159, 10.1007/s10584-006-9172-9, 2007.

606 van Vuuren D. P., Stehfest E., Gernaat D. E. H. J., Doelman J. C., van den Berg M., Harmsen M.,
607 de Boer H. S., Bouwman L. F., Daioglou V., Edelenbosch O. Y., Girod B., Kram T., Lassaletta L., Lucas
608 P. L., van Meijl H., Müller C., van Ruijven B. J., van der Sluis S. & Tabeau A.: Energy, land-use and
609 greenhouse gas emissions trajectories under a green growth paradigm, *Global Environmental Change.* 42,
610 237-250, <https://doi.org/10.1016/j.gloenvcha.2016.05.008>, 2017.

611 Westervelt D. M., Horowitz L. W., Naik V., Golaz J. C. & Mauzerall D. L.: Radiative forcing and
612 climate response to projected 21st century aerosol decreases, *Atmos. Chem. Phys.* 15(22), 12681-12703,
613 10.5194/acp-15-12681-2015, 2015.

614 Zheng B., Tong D., Li M., Liu F., Hong C., Geng G., Li H., Li X., Peng L., Qi J., Yan L., Zhang
615 Y., Zhao H., Zheng Y., He K. & Zhang Q.: Trends in China's anthropogenic emissions since 2010 as the
616 consequence of clean air actions, *Atmos. Chem. Phys.* 18(19), 14095-14111, 10.5194/acp-18-14095-
617 2018, 2018.

618

619

620

621

622

623

624

625

626

627

628

629

630

631

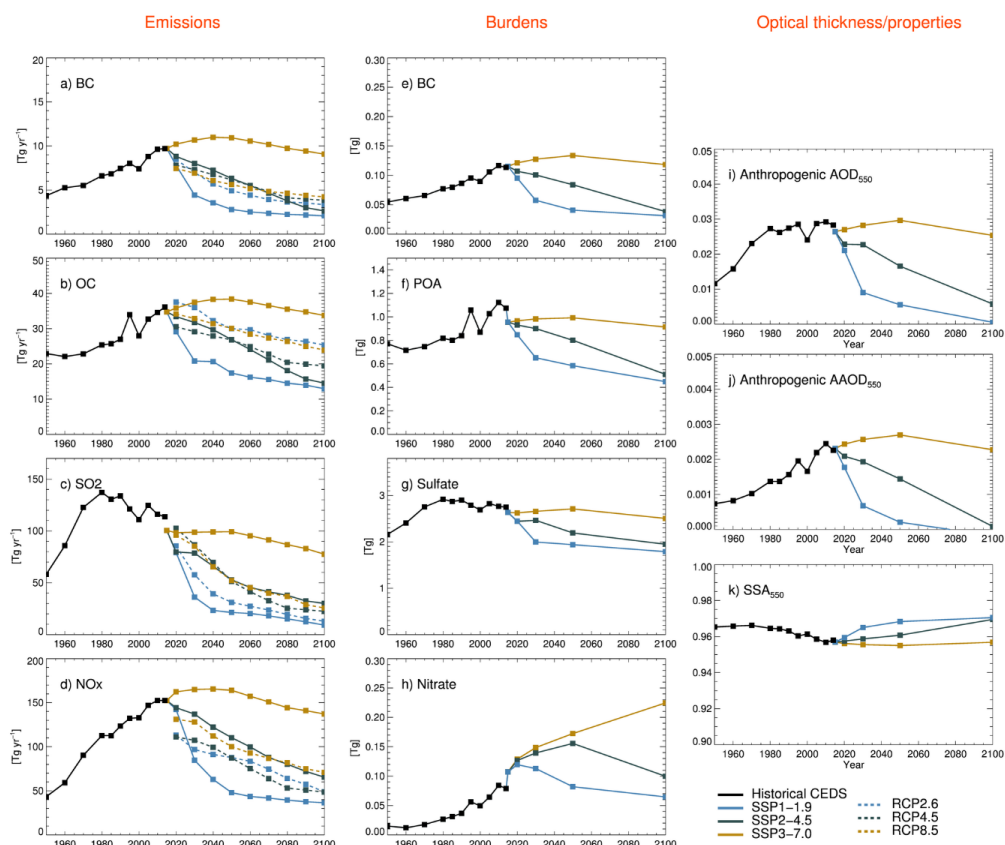
632

633

634



635 Figures

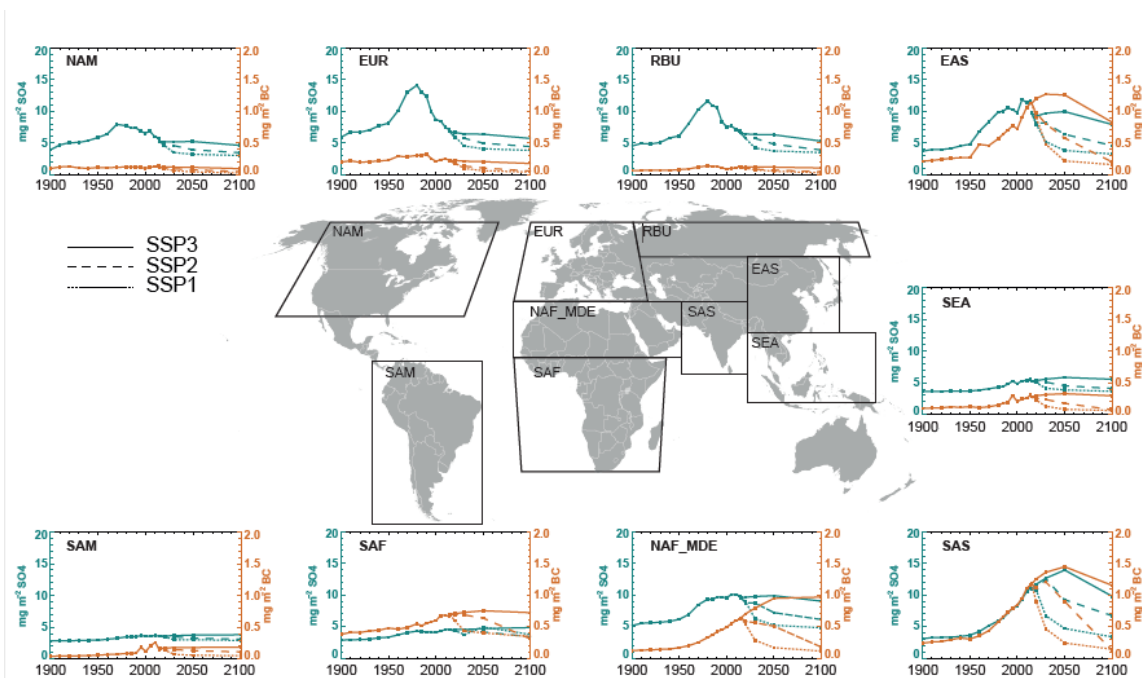


636

637 *Figure 1. Left: Annual global emissions (fossil fuel, biofuel and biomass burning) of BC, OC, SO₂ and NO_x*
 638 *over the period 1950 to 2100 from the CEDS historical inventory and SSP1-1.9, SSP2-4.5 and SSP3-7.0*
 639 *(solid colored lines). Emissions from RCP2.6, RCP4.5 and RCP8.5 (dashed lines) are added for*
 640 *comparison. Middle: Modeled total global burdens of BC, POA, sulfate and fine mode nitrate. Right:*
 641 *Anthropogenic AOD and AAOD, and total (anthropogenic and natural) SSA at 550nm.*

642

643

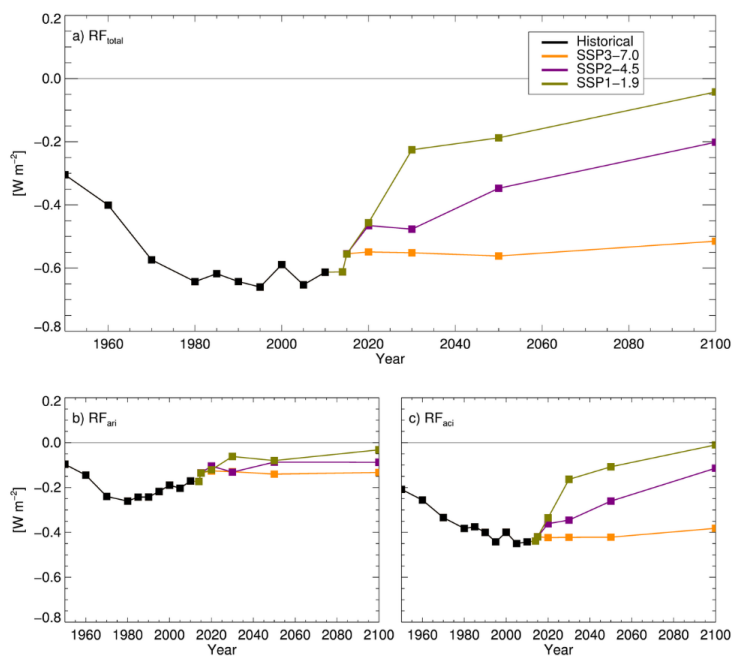


644

645 *Figure 2: Regionally averaged burdens of BC and sulfate aerosols from 1900 to 2100.*

646

647

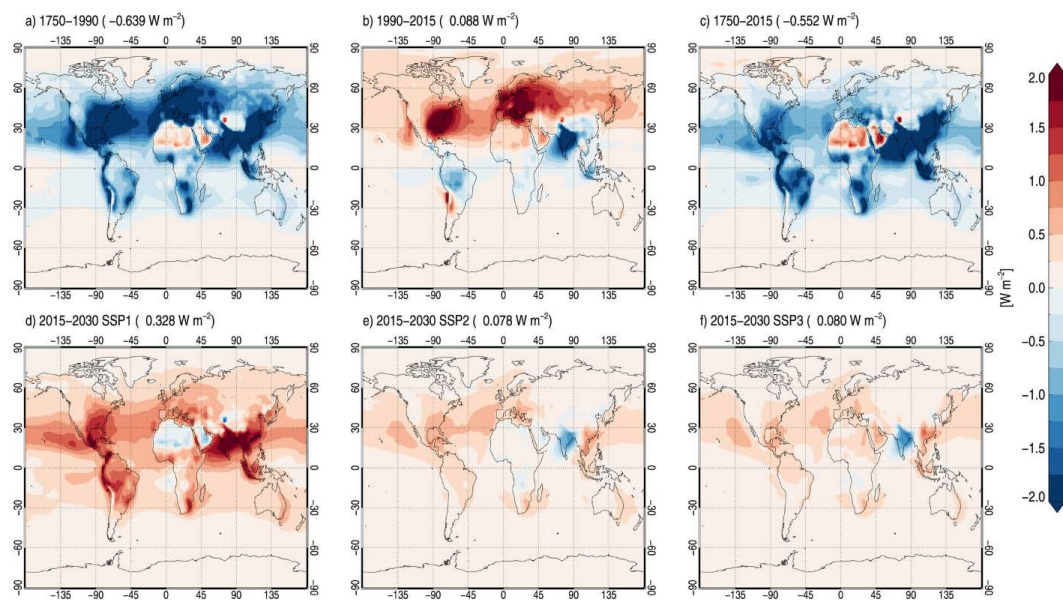


648

649 *Figure 3: Radiative forcing of anthropogenic aerosol 1950-2100 relative to 1750: a) total aerosol RF*
650 *(RF_{total}), b) aerosol-radiation interactions (RF_{ari}) and c) aerosol-cloud interactions (RF_{aci}).*

651

652



653

654 *Figure 3: Total aerosol RF over four time periods: 1750-1990, 1990-2015, 1750-2015, and 2015-2030, for*
655 *each SSP.*

656